Water Practice & Technology Vol 14 No 1
doi: 10.2166/wpt.2018.119

Monitoring water quality in Singapore reservoirs with hyperspectral remote sensing technology

S. C. Liew[a,*], C. K. Choo[b], J. W. M. Lau[c], W. S. Chan[c] and T. C. Dang[c]

[a] Centre for Remote Imaging, Sensing and Processing (CRISP), National University of Singapore, 10 Lower Kent Ridge Road, Blk S17 Level 2, Singapore 119076

[b] NexusBit Integral Pte. Ltd., Singapore

[c] PUB, Singapore's National Water Agency, Singapore

*Corresponding author. E-mail: scliew@nus.edu.sg

Abstract

In this work, algorithms were developed for retrieving water quality parameters related to Singapore's reservoirs. The main constituents that affect the water reflectance (WR) – i.e. proportion of incident light reflected from the surface of water bodies after removing the surface glint component – are the suspended particles, phytoplankton and coloured dissolved organic matter (CDOM). The existing absorption spectrum model for phytoplankton in seawater is not accurate for the phytoplankton types that exist in the fresh water environment. The phytoplankton absorption spectrum was modelled by a series of Gaussian peaks from 400 to 750 nm. The peak strengths were dynamically derived from the WR measured. The phytoplankton absorption model is incorporated into a semi-empirical WR model for retrieving the absorption and backscattering coefficients of water components such as suspended sediments, CDOM and phytoplankton. The chlorophyll-a concentration and water turbidity estimated using this model correlate well with field sampling measurements, with coefficients of determination (R^2) exceeding 0.8.

Key words: hyperspectral imaging, phytoplankton, remote sensing, turbidity, water quality

INTRODUCTION

Water quality parameters are usually obtained using in-situ sensor probes or by laboratory measurements of water samples collected on site. These conventional methods are laborious and costly, and have limited spatial coverage. Remote sensing can complement in-situ measurements with advantages of wide spatial and repetitive temporal coverage. Using remote sensing, maps showing the spatial distribution of water quality parameters can be produced at multiple time intervals for monitoring purposes. Remote sensing data can be acquired by sensors carried on satellites, as well as air-borne or ground-based platforms. In this project the implementation of near real-time area-monitoring and mapping of inland and reservoir water quality was explored using a ground-based remote sensing system. The principle and methods employed are similar to satellite imaging, and the water body naturally illuminated by sun- and/or sky-light.

When light penetrates water, it is partly absorbed, and partly scattered by water molecules and other dissolved or suspended constituents. An optical sensor deployed above the water surface can detect and measure the spectral radiance of light scattered by the water body. This carries information about the water's constituents. The constituents' optical properties (namely, the absorption and backscattering coefficients) can be derived from the detected radiance by appropriate modelling of the light/constituent interactions.

Water Practice & Technology Vol 14 No 1
doi: 10.2166/wpt.2018.119

In this project, a ground-based hyperspectral imaging (HSI) camera system developed at Lighthaus Integral was deployed for remote measurements of water radiance, which is the light reflected from the water body surface. The HSI camera operates on wavelengths from 450 to 750 nm. The spectral resolution (full width at half maximum) of each band is 15 nm. The output of the HSI camera at each scan location consists of 196 spectral data distributed over a 14×14 matrix. The sensor system is mounted on a tall building overlooking the reservoir, to achieve both wide coverage and high sampling frequency. A critical component of the monitoring system is the retrieval algorithm, which derives the optical properties of water constituents from the water reflectance (WR).

The main focus of this paper is the algorithms developed for the retrieval of chlorophyll-a concentration (Chl-a) and water turbidity data from Singapore's reservoirs. The project, which is supported by PUB, Singapore's National Water Agency, involved access to local reservoirs for in-situ measurements and water sampling for laboratory analysis of water quality parameters. The retrieval algorithms were calibrated and validated with the in-situ and laboratory measurements, together with WR data from the HSI over six months' continuous operation at the site.

RETRIEVAL ALGORITHM

There are several types of retrieval algorithm (IOCCG 2006). The earlier algorithms consist of empirical equations that correlate the reflectance or band ratios in several spectral bands to the in-situ chlorophyll concentration (Sauer *et al.* 2012). There is a limit to the applicability of such algorithms since chlorophyll is only one of many constituents that affect the inherent optical properties of water which, together with the incident radiation field, determine the WR. The recent trend has been to retrieve the inherent optical properties themselves from the WR (IOCCG 2006) as the constituents can then be related to the inherent properties using empirical relationships specific to the location and water type. A forward model is usually required for this type of algorithm to compute the WR, given the inherent optical properties as input parameters. In retrieval, the set of optical parameters that minimizes the difference between the measured and computed reflectance spectra is taken as the solution to the inverse problem. The main advantage of this method is that it is physics-based and the optical properties can be derived solely from the sensor data without any need for additional in-situ data.

The optical properties of natural freshwater are contributed by several optically active constituents: pure water, coloured dissolved organic matter (CDOM), chlorophyll in phytoplankton, and suspended particles. The forward model of WR relates the WR to the backscattering $b_b(\lambda)$ and absorption coefficients $a(\lambda)$ of water, which are modelled by Equations (1) and (2) (Lee *et al.* 1998),

$$b_b(\lambda) = b_{bw}(\lambda) + b_{bp}(\lambda) \quad (1)$$

$$a(\lambda) = a_w(\lambda) + a_g(\lambda) + a_\phi(\lambda) \quad (2)$$

where the subscripts w, p, g and ϕ refer to pure water, suspended particles, CDOM and phytoplankton respectively. The backscattering and absorption coefficients of pure water are well-known from published literature (Pope & Fry 1997). CDOM absorbs strongly in the UV to blue-green parts of the spectrum. The absorption coefficient of CDOM is usually modelled by Equation (3):

$$a_g(\lambda) = G\mathrm{e}^{-S(\lambda-440)} \quad (3)$$

where G is the value of a_g at 440 nm, an indicator of the amount of CDOM in the water, and S is the spectral slope. Suspended particles scatter light at all wavelengths and are the main factor affecting

Water Practice & Technology Vol 14 No 1
doi: 10.2166/wpt.2018.119

water turbidity. The backscattering by suspended particles is modelled using Equation (4):

$$b_{bp}(\lambda) = X(550/\lambda)^{y} \tag{4}$$

where X is the value of b_{bp} at 550 nm, which correlates strongly with turbidity, and y is a spectral shape factor.

Phytoplankton generally absorb light in the blue and red spectral regions. There is no universal model for a phytoplankton absorption coefficient as absorption by them depends on the different types and amounts of pigments present. While Chl-a is the major pigment responsible for absorption, the absorption spectrum also depends on many other factors including the sizes, types and concentrations of phytoplankton in the water. Nevertheless, the model proposed by Lee *et al.* (1998) has proved useful and is commonly used to retrieve seawater optical properties (Lee *et al.* 1998; He *et al.* 2000; Liew *et al.* 2001). In this model, phytoplankton absorption is expressed as in Equation (5):

$$a_{\phi}(\lambda) = Pa_0(\lambda) + P\ln(P)a_1(\lambda) \tag{5}$$

where P is the value of a_{ϕ} at 440 nm, an indicator for Chl-a concentration, and $a_0(\lambda)$and $a_1(\lambda)$ are empirical functions whose values are determined by fitting the measured phytoplankton absorption to the above model. Thus, the forward model for computing the WR can be represented as a nonlinear function of the three optical parameters, P, X and G, as in Equation (6):

$$R(\lambda) = f(P, X, G) \tag{6}$$

Given a measured reflectance spectrum, the retrieval process consists of finding the set of values (P, X, G) that minimizes the root-mean-square difference between the computed and measured spectra (Lee *et al.* 1998; Salinas *et al.* 2007).

The existing model for phytoplankton absorption (Equation (5)) works well for seawater. It is not sufficiently accurate, however, for the types of phytoplankton existing in the freshwater environment. In addition to the usual chlorophyll absorption peak at 674 nm, freshwater phytoplankton exhibit strong absorption peaks around 624 nm. These are not so prominent in the seawater model. Instead of using Equation (5), the phytoplankton absorption spectrum is modelled by a series of Gaussian peaks from 400 to 750 nm (Equation (7)):

$$a_{\phi}(\lambda) = \sum_{i=1}^{N} P_i \exp\left(-\frac{(\lambda - \lambda_i)^2}{2\sigma_i^2}\right) \tag{7}$$

where N is the number of Gaussian peaks in the model, λ_i the central wavelength, and σ_i the standard deviation of each Gaussian peak. The strengths P_i of these absorption peaks are retrieved dynamically from the measured WR spectra during retrieval. This phytoplankton absorption model is incorporated into a semi-empirical WR model for retrieving the absorption and backscattering coefficients of water constituents – i.e., suspended sediments, CDOM and phytoplankton. The optical properties derived from WR are then correlated with the measured turbidity, Chl-a concentration, and CDOM absorption, to establish the equations for water quality parameter retrieval from the measured WR.

METHOD

The hyperspectral sensor system was tested at two sites: one overlooking the water at the Marina Bay area of Marina Reservoir on the roof of a 140 m tall building (Jun 2016 to Aug 2017), the other overlooking the water at the intersection of Sungei Pinang and Serangoon Reservoir (Sep to Nov 2017) on

Water Practice & Technology Vol 14 No 1
doi: 10.2166/wpt.2018.119

top of a 60 m tall building. The sites have different characteristics. The Marina Reservoir was formed by constructing a dam across the Marina Channel, converting the previously saline Marina Bay into a freshwater reservoir. Its catchment includes the highly urbanized Central Business District and surrounding areas. Water quality at the Marina Bay site is quite homogenous both spatially and temporally. The Serangoon Reservoir is in north-eastern Singapore, which was developed relatively recently, and was formed by damming Sungei Serangoon at the river mouth. The Serangoon test site is located where Sungei Pinang, a tributary, drains into the main river. Water quality here is influenced by upstream runoff from Sungei Pinang and has greater variability than that at the Marina site.

The hyperspectral sensor system automatically runs a full areal scan every two hours from 0800 to 1700 daily. For each areal scan of the water, the sensor runs through 24 and 16 scan locations respectively at the Marina and Serangoon sites. Centred on each scan location, the hyperspectral imager produces a matrix of 14×14 WR measurements. At each scan location, the sensor makes three sets of radiance measurements (Figure 1): (1) total radiance L_t from the water surface; (2) sky radiance L_{sky}; and (3) radiance reflected from a reference grey surface L_{ref}.

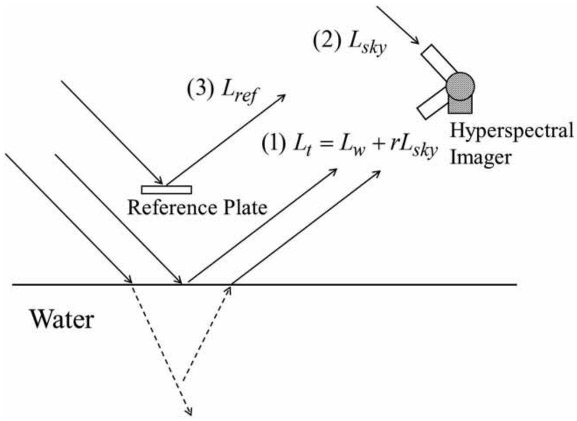

Figure 1 | Water reflectance measurement.

The WR is computed using Equation (8):

$$R(\lambda) = \frac{L_t - rL_{sky}}{kL_{ref}} \tag{8}$$

where k is a constant that compensates for the reflectance of the reference surface, and r is the Fresnel reflectance of the water surface. The reflectances are fed into the retrieval algorithm to obtain the following optical parameters: P674, P624, G440 and X550. The parameters P674 and P624 are the strengths of the Gaussian absorption peaks at 674 and 624 nm respectively (as in Equation (7)); G440 is the CDOM absorption at 440 nm and X550 the particulate backscattering coefficient at 550 nm.

Field trips were carried out during the course of the project to make in-situ measurements of water turbidity (nephelometric turbidity units – NTU) using a turbidity meter (Thermo Scientific Orion AQ3010 and Eureka Manta+ 35 Turbidity) at places corresponding to the scan locations of the hyperspectral sensor system. WR was also measured using a portable spectrometer (GER1500, Spectra Vista Corporation). Water samples were collected and sent to accredited laboratories for measurements of Chl-a and CDOM absorption. Some 20 field sampling runs – 10 each at Marina Bay and Serangoon reservoirs – were conducted, each involving visits to five sampling locations and yielding 100 data points. The batch of 50 data points from the Marina site were used for regression analysis to

Water Practice & Technology Vol 14 No 1
doi: 10.2166/wpt.2018.119

obtain the relationship between the water optical parameters and the corresponding turbidity, Chl-a concentration, and laboratory measured CDOM absorption. The 50 data points from the Serangoon site were used to verify the regression results. The regression relationships were then applied to all parameters derived from the hyperspectral sensor, to obtain the sensor-derived turbidity, Chl-a, and CDOM absorptions for the scan locations.

RESULTS

This section includes examples illustrating the procedures involved in retrieving the optical parameters from the measured WR. Figure 2 shows the WR (solid line) measured using the handheld field spectrometer at a sampling point in the Marina Reservoir on 13 July 2017. Laboratory analysis reported Chl-a concentration of 21.4 μg/l, turbidity 6.35 NTU and CDOM absorption at 440 nm of 1.14 m^{-1}.

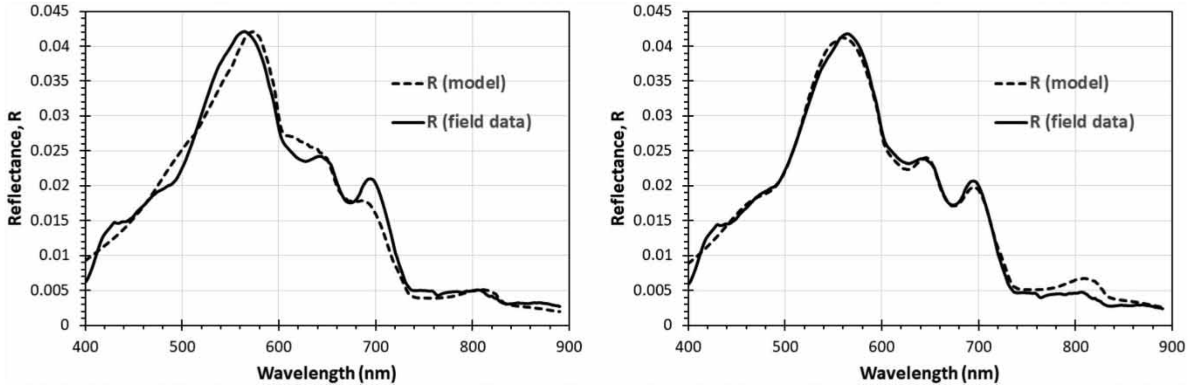

Figure 2 | Measured (solid line) and computed (dashed line) reflectance spectra at a sampling location in Marina Reservoir. The best-fit spectra are computed using the conventional phytoplankton absorption model (left panel) and the Gaussian peaks model (right panel).

The best-fit reflectance spectra (dashed lines, Figure 2), computed using the conventional phytoplankton absorption model (Equation (5)) and the Gaussian peaks model developed in this project (Equation (7)), are shown in the left and right panels of Figure 2, respectively. The measured reflectance curve clearly shows a dip around 674 nm due to absorption by Chl-a, with another, smaller, dip around 624 nm. There are further absorption features, shown as dips, around 500 and 440 nm on the shorter wavelength side. The reflectance spectrum computed using the conventional model fits the general shape of the measured spectrum but does not show the finer absorption features exhibited in the latter. The Gaussian peaks model of phytoplankton absorption, however, reproduces all of the absorption features shown in the reflectance curve.

The Gaussian peaks model of phytoplankton absorption was initially developed using measured reflectance spectra at sampling locations in Marina Reservoir and was subsequently applied to fit the reflectance curves measured at the Serangoon Reservoir site. Figure 3 shows the WR (solid line) measured at a sampling point in the Serangoon Reservoir on 20 October 2017. The laboratory reported Chl-a concentration was 16.8 μg/l, turbidity 3.22 NTU, and CDOM absorption at 440 nm 1.04 m^{-1}. The best-fit computed reflectance spectra using the two phytoplankton absorption models are also shown. Although the two reservoirs are at separate locations, the reflectance spectra have similar shapes and exhibit similar absorption features. The Gaussian peaks model fit the measured reflectance very well.

The reflectance model constructed using the Gaussian peaks model of phytoplankton absorption was then used to fit the reflectance curves obtained from the on-site ground-based hyperspectral

Water Practice & Technology Vol 14 No 1
doi: 10.2166/wpt.2018.119

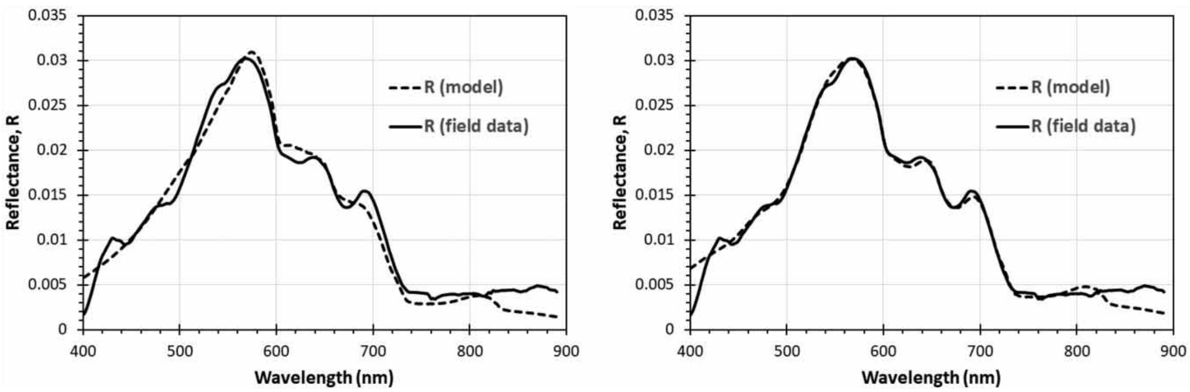

Figure 3 | Measured (solid line) and computed (dashed line) reflectance spectra at a sampling location in Serangoon Reservoir. The best-fit spectra are computed using the conventional phytoplankton absorption model (left panel) and the Gaussian peaks model (right panel).

sensor system and retrieve the reservoir water's optical parameters. Both the optical parameters P674 and P624 (i.e. the absorption coefficients of phytoplankton at 674 and 624 nm, respectively) have high correlation with the laboratory determined Chl-a concentration, with coefficients of determination (R^2) exceeding 0.8. The particulate backscattering coefficient at 550 nm (X550) also has high correlation with the water turbidity expressed in NTU, with R^2 exceeding 0.8.

The regression equations relating P674 to Chl-a and X550 to turbidity were then used to calculate the Chl-a and turbidity values from every measured reflectance spectrum. Figure 4 shows the scatter plot for the laboratory determined and remote sensor derived Chl-a, based on the water sample analyses from the 20 field trips and 5 sampling locations – i.e., 100 sampling points. The corresponding plot for water turbidity is shown in Figure 5. (Chl-a and turbidity have been normalized by their respective means in Figures 4 and 5).

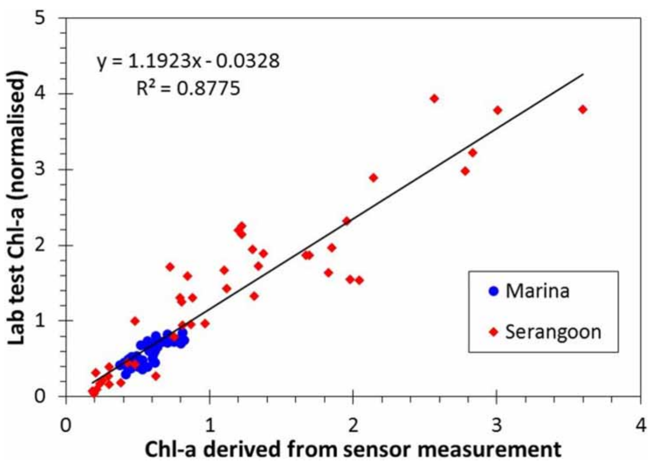

Figure 4 | Scatter plot of lab-measured and sensor-derived Chl-a (normalised to the average Chl-a value).

CDOM is usually quantified by its absorption coefficient at 440 nm. Remote sensing measurement cannot distinguish between absorption due to dissolved organic matter and organic matter present in suspended particles (detritus). Thus, the CDOM absorption reported here is the sum of the absorption due to both the dissolved and particulate organic matter. The CDOM absorption measurement reported was performed following standard laboratory absorption spectroscopy procedures (Mitchell *et al.* 2003). The scatter plot of the laboratory-measured CDOM absorption coefficient at 440 nm (G440) versus the remote sensor-derived CDOM absorption (normalized by the average value) is shown in Figure 6. An R^2 value of 0.677 is obtained after removing seven outlier points.

Water Practice & Technology Vol 14 No 1
doi: 10.2166/wpt.2018.119

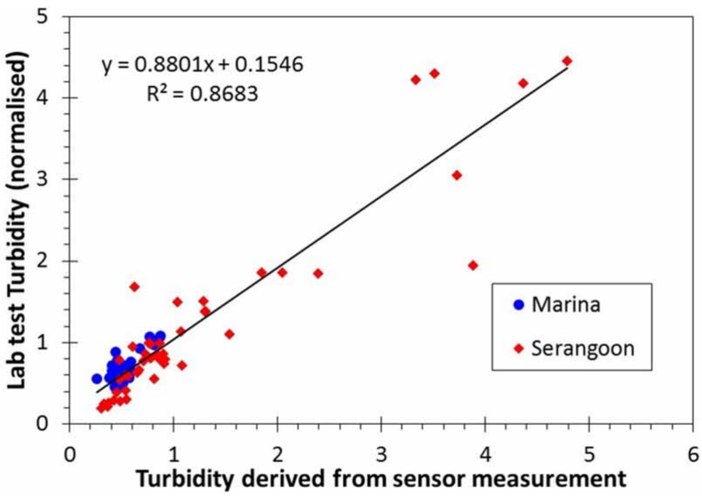

Figure 5 | Scatter plot of lab-measured and sensor-derived turbidity (normalised to the average turbidity value).

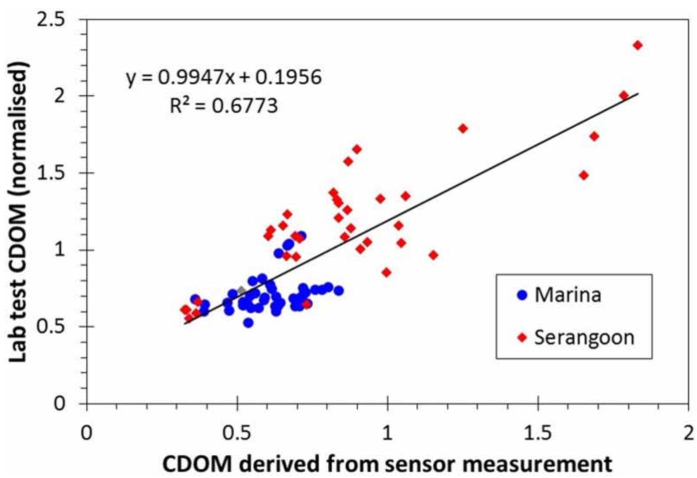

Figure 6 | Scatter plot of lab-measured and sensor-derived CDOM absorption, G440 (normalised to the average CDOM absorption value).

DISCUSSION AND CONCLUSIONS

The project demonstrated water quality parameter retrieval using a remote hyperspectral sensor system deployed on top of a high building, with wide areal coverage and high sampling frequency. The parameters Chl-a, turbidity and CDOM were monitored. Quantitative values of Chl-a (μg/l) and turbidity (NTU) could be estimated using equations obtained from regression analysis of the optical parameters derived from the remote sensor system against laboratory measured values. The sensor-derived values agree well with those reported by the laboratory, with coefficients of determination (R^2) exceeding 0.8.

An advantage of this method is that the algorithms used to derive water optical parameters from the measured WR are physics-based and no in-situ measurements are required in the retrieval procedures. The algorithms are based on well-established techniques used by the Ocean Colour Research community.

The phytoplankton absorption model (Equation (5)) that works well for seawater is not accurate for the types of phytoplankton present in reservoirs. The model could fit the general shapes of the reflectance spectra but not reproduce the finer absorption features. A Gaussian peaks model (Equation (7))

Water Practice & Technology Vol 14 No 1
doi: 10.2166/wpt.2018.119

was developed and is quite robust – i.e., it can be adapted to the different pigment compositions of different types of phytoplankton by adjusting the absorption strengths of the Gaussian peaks to fit the reflectance spectrum. The model was constructed based on the reflectance spectra collected in Marina Reservoir but performed well in fitting the WR of a different reservoir.

The optical parameters derived from remote sensor measurements are absolute physical quantities and can be regarded as indicators of the corresponding water quality parameters, i.e. P674 for Chl-a and X550 for turbidity. However, in-situ water sampling and laboratory measurements are required to relate the optical parameters to Chl-a and turbidity in the more familiar units of μg/l and NTU respectively. The relationships are expected to depend on the types of phytoplankton and suspended particles present in the water. The algorithm for sensor measurements taken over a period of more than six months, and at two different reservoirs with different characteristics, was tested in the project. The sensor-derived Chl-a and turbidity values agree with those from the laboratory with high confidence.

The results from this study could potentially lead to cost-effective and more productive methods of monitoring and mapping water quality (i.e. Chl-a, turbidity and CDOM) in open reservoirs. Remote sensing enables the mapping of relatively larger areas at higher frequency. The ground-based sensor system used in this project has limitations. For instance:

- the sensor needs to be deployed on high ground for wide coverage; and,
- system performance deteriorates at high view angle (i.e. the angle of the line of sight from the downward vertical) due to interference from external factors such as excessive surface glints and reflection.

The system generally works well for view angles of less than 60 degrees. For example, if the height of the sensor platform is 140 m, as at the Marina site, the optimal distance of coverage is about 240 m horizontally from the sensor location.

The system developed for this project, consisting of sensor hardware and retrieval algorithms, could be adapted for deployment in different platform configurations. A drone-based system flying over water bodies could map surface water quality variations without the constraint of view angle, for instance.

REFERENCES

He, M. X., Liu, Z. S., Du, K. P., Li, L. P., Chen, R., Carder, K. L. & Lee, Z. P. 2000 Retrieval of chlorophyll from remote-sensing reflectance in the China seas. *Applied Optics* **39**(15), 2467–2474.

IOCCG. 2006 *Remote Sensing of Inherent Optical Properties: Fundamentals, Tests of Algorithms, and Applications* (Lee, Z. P. ed.). IOCCG, Dartmouth, Canada.

Lee, Z. P., Carder, K. L., Mobley, C. D., Steward, R. G. & Patch, J. S. 1998 Hyperspectral remote sensing for shallow waters. I. A semi-analytical model. *Applied Optics* **37**(27), 6329–6338.

Liew, S. C., Lim, K. H. & Kwoh, L. K. 2001 Retrieval of chlorophyll absorption spectra from remote sensing reflectance of turbid coastal waters. *Proc. 2001 IEEE International Geoscience and Remote Sensing Symposium* **1**, 284–286.

Mitchell, B. G., Kahru, M., Wieland, J. & Stramska, M. 2003 Determination of spectral absorption coefficients of particles, dissolved material and phytoplankton for discrete water samples. In: *Ocean Optics Protocols for Satellite Ocean Color Sensor Validation*. NASA/TM-2003-211621/Rev4-Vol. IV. Greenbelt, Maryland, pp. 39–64.

Pope, R. M. & Fry, E. S. 1997 Absorption spectrum (380–700 nm) of pure water. II. Integrating cavity measurements. *Appl. Opt.* **36**, 8710–8723.

Salinas, S. V., Chang, C. W. & Liew, S. C. 2007 Multiparameter retrieval of water optical properties from above-water remote-sensing reflectance using the simulated annealing algorithm. *Applied Optics* **46**(14), 2727–2742.

Sauer, M. J., Roesler, C. S., Werdell, P. J. & Barnard, A. 2012 Under the hood of satellite empirical chlorophyll a algorithms: revealing the dependencies of maximum band ratio algorithms on inherent optical properties. *Optics Express* **20**(19), 20920–20933.